

Investigation of the homogenisation behaviour of Nd–Fe–Nb–B alloys

F.M. Ahmed, D.S. Edgley, I.R. Harris

School of Metallurgy and Materials, The University of Birmingham, Edgbaston, Birmingham B15 2TT, UK

Received 2 November 1994

Abstract

In order to establish the role of Nb–Fe–B precipitates, generated in the microstructure upon the addition of Nb to the stoichiometric Nd–Fe–B alloy, three alloys: $\text{Nd}_{11.8}\text{Fe}_{82.3}\text{B}_{5.9}$ (A), $\text{Nd}_{11.8}\text{Fe}_{81.3}\text{Nb}_1\text{B}_{5.9}$ (B) and $\text{Nd}_{11.8}\text{Fe}_{80.3}\text{Nb}_2\text{B}_{5.9}$ (C) were characterised by studying the changes in the microstructure, the electrical resistivity and the microhardness during homogenisation.

The microstructure of the as-cast alloys contains: $\text{Nd}_2\text{Fe}_{14}\text{B}$ matrix phase (ϕ), Nd-rich phase, free iron and in alloys B and C $\text{Nb}_{26}\text{Fe}_{32}\text{B}_{42}$ ternary phase. When alloys B and C are homogenised they contain predominantly ϕ and $\text{Nb}_{26}\text{Fe}_{32}\text{B}_{42}$ with only very small amounts of the Nd-rich material. $\text{Nb}_{26}\text{Fe}_{32}\text{B}_{42}$ was found to nucleate within the free iron, providing strong evidence for the role of Nb in the removal of free iron from the microstructure.

The electrical resistivity and the microhardness of the alloys were measured at regular intervals during the homogenisation process at 1000 °C. These studies revealed that, after 90 h, alloy B was homogenised completely and alloy C was homogenised after 40 h; this was in good agreement with the microstructural studies. The resistance measurements also indicated a degree of anisotropy in the as-cast material. At an intermediate stage, both alloys exhibit maxima in the resistance and microhardness curves which could indicate an age hardening process.

Keywords: Homogenisation behaviour; Electrical resistivity; Microhardness

1. Introduction

Nd–Fe–B magnets have excellent magnetic properties but their remanence and their intrinsic coercivity reduce rapidly on heating. In addition, commercial magnets such as $\text{Nd}_{15}\text{Fe}_{77}\text{B}_8$ tend to corrode readily in humid and oxidising atmospheres because of the presence of the Nd-rich phase and to some extent the $\text{Nd}_{1+x}\text{Fe}_4\text{B}_4$ phase in the microstructure of these magnets [1–3]. These limitations make such magnets useful only well below their Curie temperature (≈ 310 °C) and in non-reactive dry atmospheres. An important objective therefore, is to make these magnets more suitable for applications at elevated temperatures and in corrosive environments. Several approaches have been adopted to improve the temperature stability and the corrosion resistance of these magnets, see for example [4–8]. Many elements (e.g. Dy, Al, Co) have been added to increase room temperature coercivity so that the magnet can still achieve high coercivity values at elevated temperatures [6,7]; some of these elements, for example Al, Cu, Sn, Zn, also form eutectic phases at the grain boundaries obstructing the oxidation of Nd-rich phase

and improving the corrosion resistance [7,8]. Alternative elements such as Nb, Zr, have been added to try to change the coercivity mechanism to a pinning mechanism [9–12]. This approach has not yet been successful. The effect of niobium addition on the Nd–Fe–B alloys and magnets has been reviewed previously [13].

In this paper the effect of the addition of niobium to stoichiometric compositions, according to the formula $\text{Nd}_{11.8}\text{Fe}_{82.3-x}\text{Nb}_x\text{B}_{5.9}$ was investigated with a view to understand the homogenisation behaviour and the phase relationships. This is a necessary precursor to the possible production of magnets based on these compositions which avoid the problems associated with preferentially corroding phases. The electrical resistivity and microhardness measurements were used in this investigation to monitor the homogenisation process. Previously such measurements have been closely correlated with changes in coercivity in 2-17 type alloys [14,15].

2. Experimental procedure

The alloys $\text{Nd}_{11.8}\text{Fe}_{82.3}\text{B}_{5.9}$ (A), $\text{Nd}_{11.8}\text{Fe}_{81.3}\text{Nb}_1\text{B}_{5.9}$ (B) and $\text{Nd}_{11.8}\text{Fe}_{80.3}\text{Nb}_2\text{B}_{5.9}$ (C) investigated in the

present study, were supplied by Rare Earth Products, UK. These alloys were homogenised under a vacuum for times up to 120 h, in 10 h intervals, at temperatures of 1000, 1050 and 1100 °C and then furnace cooled. Samples prepared from the as-cast and homogenised alloys were characterised using backscattered electron imaging on a Joel 5200 SEM.

Electrical resistivity measurements at room temperature were carried out after each homogenisation stage, in order to see if there was a relationship between the homogenisation conditions and the measured electrical resistance. The apparatus used to measure the electrical resistance of specimens was based on the standard four probe method, which requires a symmetrical sample having uniform cross-sectional area with four attached leads. The principle of this method is to pass a known current (in this case 1 A) through the sample and to record the voltage drop across a specific distance. Since the voltage and the current are known, the resistance and the resistivity of the sample can be calculated by applying Ohm's law. Each resistivity measurement was performed on four samples, each of which were measured 8 times (i.e. a mean of 32 values was used), the error value quoted is one standard deviation. Microhardness measurements were made on the matrix phase of the alloys after each stage of homogenisation using a "Leitz" microhardness tester. Care was taken both to avoid microcracks during the indentation tests and also to avoid areas of the grain boundary phase. A mean of eight microhardness values was used in this work.

3. Results and discussion

3.1. Microstructural studies

The microstructure of the as-cast stoichiometric $\text{Nd}_2\text{Fe}_{14}\text{B}$ alloy (A) is shown in Fig. 1. It proved to be heterogeneous with three phases: (a) the matrix (ϕ) phase, (b) a large volume fraction of free iron and (c) the Nd-rich phase. The free iron (b), retained during a nonequilibrium cooling of the ingot, would have a detrimental influence on the magnetic properties because it serves as a nucleation site for reverse domains during magnetisation reversal. Fig. 2, shows the microstructure of the as-cast B alloy. It has another phase in addition to the phases present in alloy A. The fourth phase is the Nb–Fe–B ternary phase (d) which can be seen within the free iron phase. The microstructure of the as-cast C alloy is shown in Fig. 3, and consists of the same phases found in alloy B but with a higher volume fraction of the Nb–Fe–B phase. The composition of the Nb–Fe–B ternary phase was determined previously to be $\text{Nb}_{26}\text{Fe}_{32}\text{B}_{42}$ [13].



Fig. 1. Back-scattered electron image of the as-cast stoichiometric $\text{Nd}_{11.8}\text{Fe}_{82.3}\text{B}_{5.9}$ (A) alloy: (a) matrix 2-14-1 phase; (b) free iron; (c) Nd-rich phase.



Fig. 2. Back-scattered electron image of the as-cast $\text{Nd}_{11.8}\text{Fe}_{81.3}\text{Nb}_1\text{B}_{5.9}$ (B) alloy: (a) matrix 2-14-1 phase; (b) free iron; (c) Nd-rich phase; (d) Nb–Fe–B ternary phase.

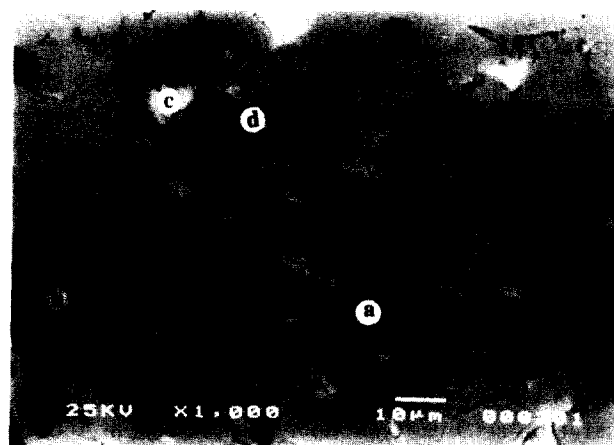


Fig. 3. Back-scattered electron image of the as-cast $\text{Nd}_{11.8}\text{Fe}_{80.3}\text{Nb}_2\text{B}_{5.9}$ (C) alloy: (a) matrix 2-14-1 phase; (b) free iron; (c) Nd-rich phase; (d) Nb–Fe–B ternary phase.

Homogenisation of alloy A for 120 h at 1000 °C was found to be insufficient to remove all the free iron, (see Fig. 4). The optimum homogenisation conditions were found to be 90 and 40 h at 1000 °C for alloys B and C respectively. (1000 °C was chosen as at higher temperatures the alloys were found to react with the stainless steel sheet in which they were wrapped). Figs. 5 and 6 show the microstructure of the homogenised B and C alloys; both alloys contain basically two phases, (a) the matrix (ϕ) phase and (b) the $\text{Nb}_{26}\text{Fe}_{32}\text{B}_{42}$ ternary phase. The dendritic free iron in the as-cast condition has been eliminated and the Nb–Fe–B phase can be observed as platelet or needle-like precipitates. In addition, the Nd-rich phase (c) is reduced to a very small amount (perhaps due to a solid–liquid reaction that leads to the formation of the ϕ phase). The $\text{Nd}_{1+x}\text{Fe}_4\text{B}_4$ boride phase was not observed either in the as cast or the homogenised alloy.

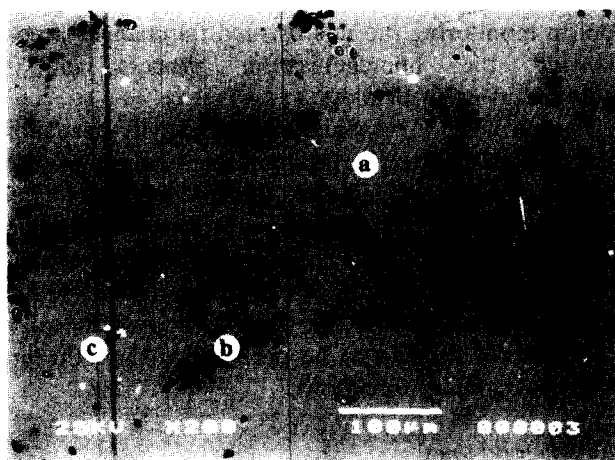


Fig. 4. Back-scattered electron image of the incompletely homogenised (120 h at 1000 °C) stoichiometric $\text{Nd}_{11.8}\text{Fe}_{82.3}\text{B}_{5.9}$ (A) alloy: (a) matrix 2-14-1 phase; (b) free iron; (c) Nd-rich phase.

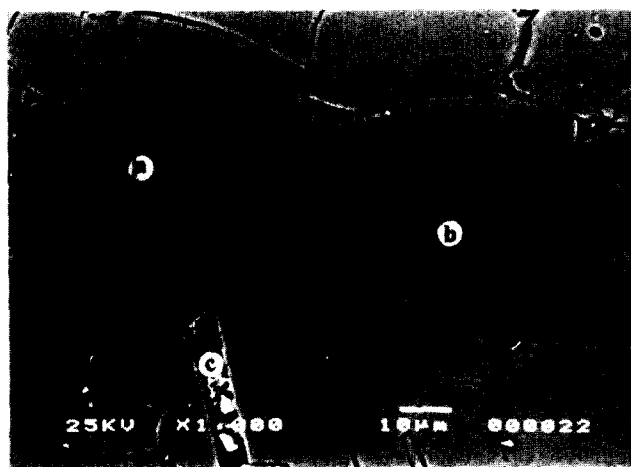


Fig. 5. Back-scattered electron image of the homogenised (for 90 h at 1000 °C) $\text{Nd}_{11.8}\text{Fe}_{81.3}\text{Nb}_1\text{B}_{5.9}$ (B) alloy: (a) matrix 2-14-1 phase; (b) Nb–Fe–B ternary phase; (c) Nd-rich phase.

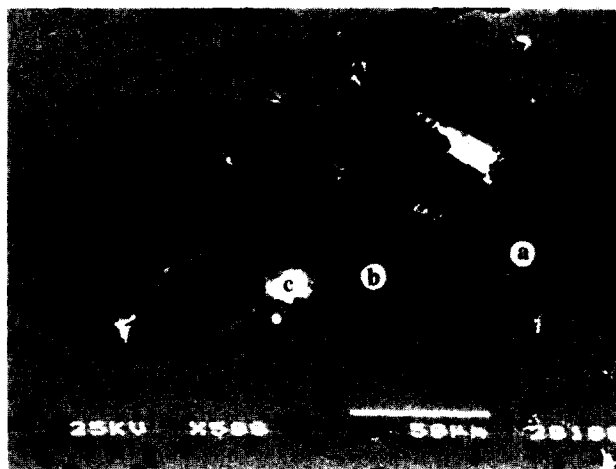


Fig. 6. Back-scattered electron image of the homogenised (for 40 h at 1000 °C) $\text{Nd}_{11.8}\text{Fe}_{80.3}\text{Nb}_2\text{B}_{5.9}$ (C) alloy: (a) matrix 2-14-1 phase; (b) Nb–Fe–B ternary phase; (c) Nd-rich phase.

After homogenisation, the solubility of niobium in the matrix phase of alloys B and C was studied by analyzing the Nb content in the matrix phase, using electron probe microanalysis (EPMA) and was found to be 0.31 at.% and 0.36 at.% respectively [16].

Zhang [17] found that homogenisation of $\text{Nd}_2\text{Fe}_{14}\text{B}$ and $\text{Nd}_{2.05}\text{Fe}_{14}\text{B}$ alloys at 1060 °C for 13 days could not remove the free iron from the microstructure. He also found that by cycling the homogenisation (heating the samples to 1140 °C for 1 h then holding at 1050 °C for 2 h and repeating this cycle) of near stoichiometric samples the removal of iron was achieved. The time required for the cyclic homogenisation of both alloys was about 120 h; this is much quicker than homogenisation at constant temperature.

Chang et al. [18] found that a similar near ϕ phase composition required 92 h at 1000 °C to reduce the free iron to less than 2%. Chang's estimated homogenisation times were based on the image analysis of the iron phase; this may sometimes be misleading as it depends on the sectioning of the alloy. Zhang [17] suggested that thin slab casts tend to produce very fine dendrites and usually required shorter homogenisation times. Even with very thin slab casts however, Zhang [17] found that under constant temperature homogenisation it was not possible to remove all the free iron.

In the present work the addition of Nb to the stoichiometric alloys (B and C) has been shown to reduce the homogenisation times significantly. This is because of the consumption of the free iron by the Nb-containing phase as explained by the model presented in our previous work [13]. Alloy C, which contains more Nb, was found to homogenise much faster than alloy B and this can be explained by the greater availability of Nb atoms. However, Nb additions in excess of 2 at.% (in the stoichiometric alloy) [16] and 3 at.% (for the alloy containing a larger amount of

the Nd-rich phase) [12] destabilise $\text{Nd}_2\text{Fe}_{14}\text{B}$ causing the formation of the $\text{Nd}_2\text{Fe}_{17}$ phase.

3.2. Electrical resistivity

Fig. 7 shows the electrical resistivity behaviour for the three alloys, A, B and C. For alloy A there is an initial sharp increase in resistivity after 10 h of homogenisation and after this the resistivity increases at a decreasing rate up to 80 h followed by a slight increase after 90 h and a small decrease after 120 h. This increase in electrical resistivity is related closely to the rate at which free iron is disappearing from the mi-

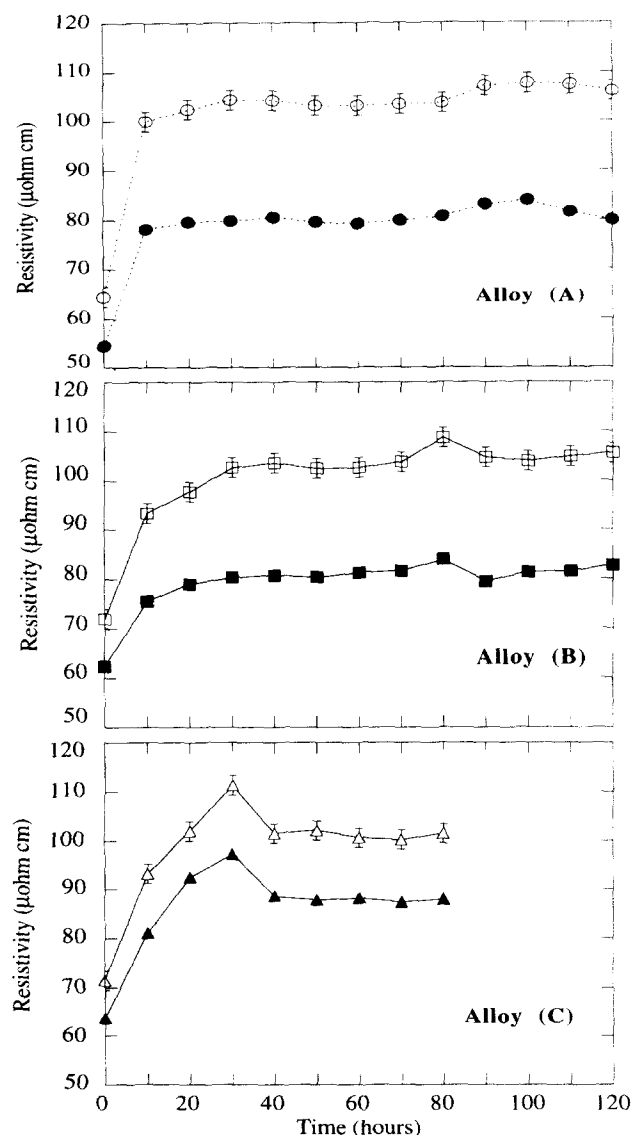


Fig. 7. Electrical resistivity vs. time during homogenisation (at 1000 °C) of the alloys: $\text{Nd}_{11.8}\text{Fe}_{82.3}\text{B}_{5.9}$ (A) alloy; $\text{Nd}_{11.8}\text{Fe}_{81.3}\text{Nb}_1\text{B}_{5.9}$ (B) alloy; $\text{Nd}_{11.8}\text{Fe}_{80.3}\text{Nb}_2\text{B}_{5.9}$ (C) alloy. The magnitude of the error bars are the same for the three alloys. The magnitude of the error bars are the same for the three alloys. Open symbols indicate current \perp to cooling direction. Full symbols indicate current \parallel to cooling direction.

crostructure. The smaller changes in resistivity after prolonged homogenisation can be explained by the slow consumption of free iron due to the relatively long diffusion distances between the free iron and the Nd-rich material, (see Fig. 4).

The electrical resistivity increases with the homogenisation time and reaches a maximum after 80 h for alloy B and 30 h for alloy C. Prolonged ageing times, for alloys B and C, (after 90 and 40 h respectively), were shown to have little effect upon the electrical resistivity. From the microstructural observations of alloys B and C, it was determined that the free iron is removed completely after 90 and 40 h of homogenisation respectively. Therefore, the resistance studies are consistent with the microstructural observations. Additionally, the maximum resistivity values after 30 and 80 h of homogenisation can be related to an age hardening phenomenon associated with precipitation of the $\text{Nb}_{26}\text{Fe}_{32}\text{B}_{42}$ ternary phase. In this work, electrical resistivity measurements have proven to be a useful tool in monitoring the microstructural changes accompanying the homogenisation process in the $\text{Nd}_{11.8}\text{Fe}_{82.3-x}\text{Nb}_x\text{B}$ alloys.

Furthermore, a comparison of resistivity perpendicular and parallel to the predominant cooling direction in the as-cast alloys, indicates that the resistivity values in the perpendicular direction are consistently higher. This consistent difference in resistivity indicates a degree of anisotropy and could be due to a preferred orientation of the ϕ phase during the solidification of the alloys (the c-axis is thought to be perpendicular to the predominant cooling direction).

3.3. Microhardness

The mean microhardness of the as-cast alloys was 764 ± 30 VHN for alloy A, 840 ± 28 VHN for alloy B and 870 ± 29 VHN for alloy C. Fig. 8 shows the variation in the microhardness behaviour of alloys A, B and C during homogenisation at 1000 °C. (The microhardness results were divided by the as-cast microhardness values in order to relate the changes in microhardness to the homogenisation process.) The matrix microhardness for alloy A increased sharply until 60 h of homogenisation and then increased at a slower rate, reaching a maximum after 110 h. The microhardness for alloy A behaved in a somewhat similar manner to the electrical resistivity curve and therefore the explanation given in section B could also be valid here.

It can be seen that the matrix microhardness increases with time up to a maximum after 80 and 30 h, for alloys B and C respectively, followed by a gradual decrease on subsequent heat treatment. These changes in the microhardness upon homogenisation can be ascribed to the removal of the free iron and growth of the Nb–Fe–B phase. For alloys B and C, it is

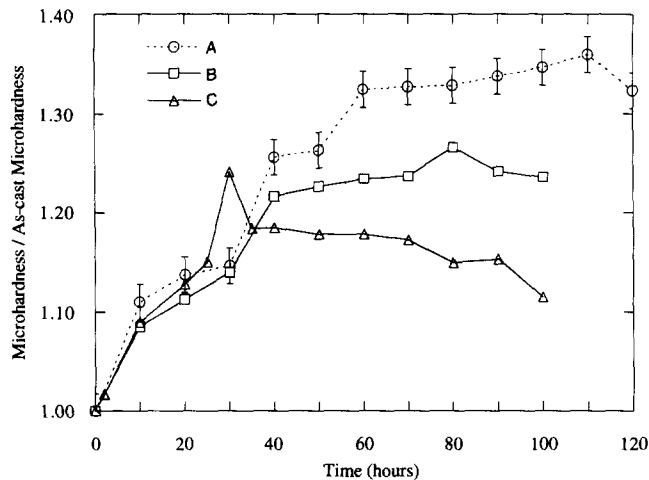


Fig. 8. Changes in microhardness vs. time during homogenisation (at 1000 °C) of the alloys: $\text{Nd}_{11.8}\text{Fe}_{82.3}\text{B}_{5.9}$ (A) alloy, $\text{Nd}_{11.8}\text{Fe}_{81.3}\text{Nb}_1\text{B}_{5.9}$ (B) alloy and $\text{Nd}_{11.8}\text{Fe}_{80.3}\text{Nb}_2\text{B}_{5.9}$ (C) alloy.

interesting to note that the microhardness peaks correspond with the peaks in the electrical resistivity curves and both effects can be attributed to an age hardening phenomenon associated with the Nb–Fe–B phase.

4. Conclusions

- (1) Nb contributes significantly to the homogenisation of the alloys by reacting with free iron and boron to produce the $\text{Nb}_{26}\text{Fe}_{32}\text{B}_{42}$ ternary phase. This reduces the time required for homogenisation at 1000 °C when compared with that of the standard $\text{Nd}_2\text{Fe}_{14}\text{B}$ alloy. The greater the Nb addition (< 3 at.%) the shorter the homogenisation time.
- (2) For alloys B and C the microhardness results followed the same trend as the resistance results and both indicated the possibility of an age hardening phenomenon caused by the growth of the $\text{Nb}_{26}\text{Fe}_{32}\text{B}_{42}$ ternary phase.
- (3) Electrical resistivity and microhardness measurements have been demonstrated to be an effective means of studying the homogenisation process in these alloys.

Acknowledgements

The authors would like to thank G. Mycock of Rare Earth Products for supplying the materials and for useful discussions. Thanks are due to the Libyan Secretariat of Scientific Research and Development for

provision of a research scholarship for F.M. Ahmed. SERC and the European Commission are acknowledged for the support of the general research programme of which this work forms a part. Thanks are also extended to O. Gutfleisch for his help with the resistivity measurements.

References

- [1] S. Szymura, H. Bala, G. Pawlowska, Yu.M. Rabinovich, V.V. Sergeev and D.V. Porkovskii, *J. Less-Common Met.*, **172**, 2 (1991) 185.
- [2] F.E. Camp and A.S. Kim, Effect of microstructure on the corrosion behaviour of NdFeB and NdFeCoAl magnets, *J. Appl. Phys.*, **70** (1991) 6348.
- [3] H. Bala, S. Szymura and J.J. Wyslocki, Corrosion characteristics of $\text{Nd}_2\text{Fe}_{14-x}\text{Ni}_x\text{B}$ permanent magnets, *IEEE Trans. Magn.*, **26** (5) (1990) 2646.
- [4] T. Shimoda, K. Akioka, O. Kobayashi, T. Yamagami, *J. Appl. Phys.*, **64** (1988) 5290.
- [5] M. Sagawa, P. Tenaud, F. Vial and K. Hiraga, *IEEE Trans. Magn.*, **26** (1990) 1957.
- [6] S. Hirota, A. Hanaki, H. Tomizawa, S. Mino and A. Hamamura, *IEEE Trans. Magn.*, **26** (1990) 1960.
- [7] Y. Xiao, S. Liu, H.F. Mildrum, K.J. Strnat and A.E. Ray, The effects of various alloying elements on modifying the elevated temperature magnetic properties of sintered Nd–Fe–B magnets, *J. Appl. Phys.*, **63** (8) (1988) 3516.
- [8] J. Fidler, Two types of dopant with different microstructural effects leading to an improvement of rare earth–iron based magnets, *7th Int. Symp. on Magnetic Anisotropy and Coercivity in RE–TM Alloys*, Canberra, July 16, 1992, p. 11.
- [9] S.F. Parker, P.J. Grundy and J. Fidler, Electron microscope study of precipitation in a Nb-containing (Nd,Dy)–Fe–B sintered magnet, *J. Magn. Magn. Mater.*, **66** (1987) 74.
- [10] S.F. Parker, R.J. Pollard, D.G. Lord and P.J. Grundy, Precipitation in NdFeB-type magnet materials, *IEEE Trans. Magn.*, **23** (5) (1987) 2103.
- [11] T. Ishikawa, Y. Hamada and K. Ohmori, Domain wall pinning by fine precipitates, *IEEE Trans. Magn.*, **25** (5) (1989) 3434.
- [12] W. Rodewald, and B. Wall, Structure and magnetic properties of sintered Nd–Fe–Nb–B magnets, *J. Magn. Magn. Mater.*, **80** (1989) 57.
- [13] F.M. Ahmed, D.S. Edgley and I.R. Harris, Effect of niobium addition on the Nd–Fe–B alloy and magnet, *J. Alloys Compounds*, **209** (1994) 363.
- [14] A. Kianvash and I.R. Harris, Coercivity dependence of a $\text{Sm}_2(\text{Co}, \text{Fe}, \text{Cu}, \text{Zr})_{17}$ type alloy on magnetic processing procedure, *J. Mater. Sci.*, **19** (1984) 353.
- [15] F. Gencer, *Ph.D. Thesis*, University of Birmingham, 1990.
- [16] F.M. Ahmed, D.S. Edgley and I.R. Harris, Effect of initial microstructure on the HDDR behaviour of the Nd–Fe–Nb–B stoichiometric alloys, *Proc. of the 13th Int. Workshop on R–E Magn. and their Appl.*, Birmingham, September 11–14, 1994, pp. 463.
- [17] X.J. Zhang, *Ph.D. Thesis*, University of Birmingham, 1991.
- [18] W.C. Chang, T.S. Chin and K.S. Liu, The dissolution kinetics of free iron in Nd–Fe–B permanent magnet alloys, *J. Magn. Magn. Mater.*, **80** (1989) 352.